Towards more accurate reservoir imaging using FWI: an OBN case study at Trion

Zhen Wang, Sen Mei, Zhuocheng Yang, (CGG); Joakim Blanch, Ezequiel Genova, Juan-Mauricio Florez-Nino (BHP); Humberto Salazar-Soto, Alfredo Vazquez-Cantu (PEMEX)*

Summary

The Trion field in the western Gulf of Mexico (GoM) exhibits folded sediment beddings and strong attenuation bodies, which pose great challenges for seismic imaging. After a decade of processing effort employing the latest imaging technology, the available towed-streamer data for this area hit a technical limit. Improvements to velocity models and images were incremental, and it was determined that better data were needed to make a step change in image quality. To this end, an ocean bottom node (OBN) acquisition was carried out in late 2020 to record full-azimuth and long-offset seismic data with good low-frequency content. Time-lag FWI (TLFWI) using this OBN data was able to improve the tilted orthorhombic (T-ORT) velocity models, which led to better migrated images from least-squares (LS) Kirchhoff and reverse time migration (RTM). However, the reservoir image below the shallow absorption anomalies remained unsatisfactory. As an alternative imaging product, the FWI Image from TLFWI showed better structural continuity and more coherent amplitudes at the reservoir than LS-Kirchhoff or LSRTM.

Introduction

Discovered in 2012, the Trion deep-water field is located within the Perdido Fold Belt in the western GoM, approximately 30 km south of the US-Mexico maritime border and approximately 180 km away from the Mexican coastline. The field lies in a water depth of 2500 m and covers an area of approximately 20 km^2. It comprises heavily faulted and folded sediments, shale bodies, and multiple shallow low-velocity absorption anomalies above the reservoir section. This geologically complex setting results in several imaging challenges, including the presence of orthorhombic anisotropy and weak amplitudes below the shallow absorption anomalies.

Over the last decade, multiple attempts were made to improve the reservoir image at Trion. The most recent processing attempt was conducted in 2019 with two wide-azimuth towed-streamer (WAZ) data sets and a narrow-azimuth towed-streamer (NAZ) data set using TLFWI (Zhang et al., 2018; Wang et al., 2019) and LS-Kirchhoff (Shuster, 1993) for velocity update and imaging. While the 2019 streamer processing product provides good resolution, the image at Trion is still suboptimal (Figure 1). The events at the reservoir level (yellow circle in Figure 1a) are incoherent and the amplitude map extracted at the top of the reservoir (Figure 1b) is noisy and non-geological.

An OBN survey was carried out in late 2020 at Trion to further improve the velocity and image. The OBN data is ideal for velocity updates with FWI due to its full-azimuth, long-offset coverage, and great low-frequency content. Many successful examples have been reported using TLFWI and OBN data to achieve better velocity and imaging (Nolte et al., 2019; Yao et al., 2020). In this study, we followed a similar data-driven approach for TLFWI application with OBN data. The improved velocity model derived from TLFWI resulted in a substantial uplift in the reservoir imaging.

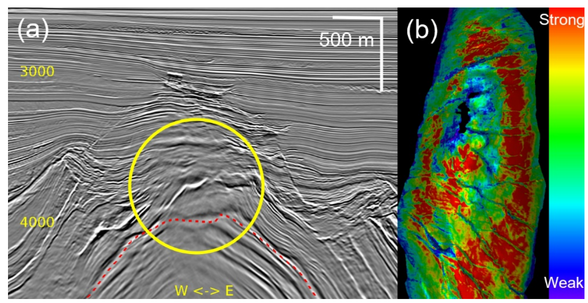

Figure 1: (a) 2019 legacy LS Q Kirchhoff stack at the Trion reservoir. The top of the reservoir (trough) is indicated by the dashed red line, and its trough amplitude is plotted in (b). The structural image below the shallow anomalies is incoherent (yellow circle in a) and non-geological dim zones are observed on the amplitude horizon in (b).

OBN data

The OBN data were acquired with up to 30 km offsets and three different node spacing layouts: 200 x 200 m, 400 x 400 m, and 800 x 800 m (Figure 2), where the densest nodes cover the reservoir area and the sparse nodes are designed for velocity model building over the Trion field. The survey utilized a rolling node spread where a minimum 12.5 km

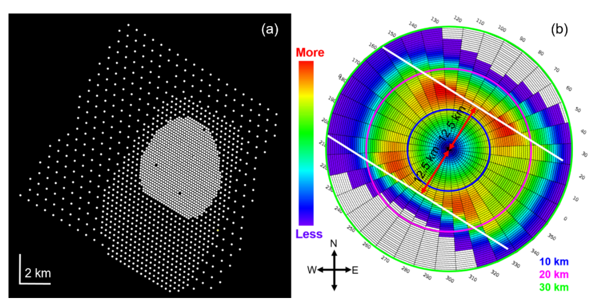

Figure 2: Trion OBN survey (a) node map and (b) rose diagram. OBN nodes are indicated by white dots, showing 200 x 200 m spacing, 400 x 400 m spacing, and 800 x 800 m spacing node coverage. The rose diagram is plotted with max offset of 30 km.

crossline offset was maintained. The diving wave illumination (Ahmed, 2018) of the acquired OBN data is more uniform and deeper than the two WAZ data sets used in the 2019 processing due to full-azimuth coverage and long offsets (Figure 3).

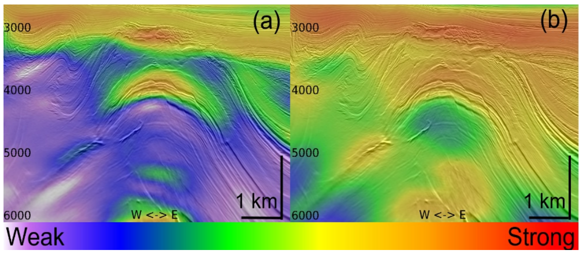

Figure 3: Diving wave illumination overlaid on the Kirchhoff stack from (a) the two WAZ data sets combined and (b) the OBN data set.

T-ORT TLFWI with OBN data

Due to the presence of substantial azimuthal velocity heterogeneity, tilted orthorhombic is needed to address the strong velocity anisotropy at Trion. A T-ORT model uses nine parameters to describe the P-wave velocity field (Tsvankin, 1997). In legacy 2019 processing, T-ORT anisotropy parameters were derived from azimuthally sectored TTI models generated from ray-based reflection tomography in the respective individual azimuths using two WAZ data in EW and NS directions. Then T-ORT TLFWI (7 Hz) for velocity update was performed using EW and NS WAZ data. It is difficult for ray-based tomography to address the complex velocity variations for estimating T-ORT parameters at Trion field. The unresolved lateral velocity variation can affect the accuracy of the orthorhombic parameters and hence affect the velocity update from TLFWI. In this study, we started from smoothed 2019 velocity model and used a TLFWI-driven orthorhombic model building approach (Shao et al., 2020) to capture the complex velocity variations and azimuthal anisotropy. We performed 6 azimuthally sectored TTI TLFWIs to update v_0 using the data in their corresponding azimuth sectors, all starting from the same initial TTI model. The updated TTI models were able to flatten gathers in their corresponding azimuths. The Trion T-ORT model was then projected from these 6 TTI models.

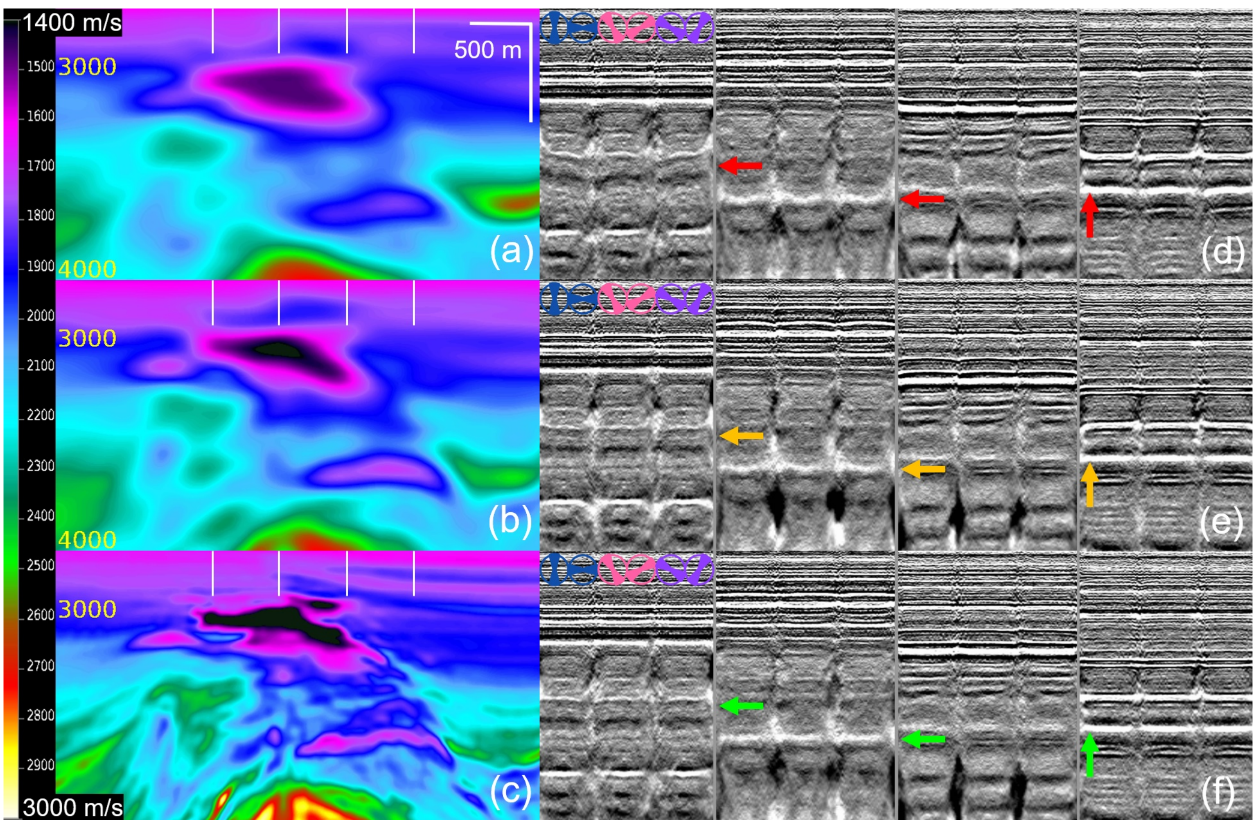

Figure 4: Three models and corresponding OBN Kirchhoff gathers. (a) 2017 TTI model, (b) 2019 T-ORT model from 7 Hz streamer TLFWI, and (c) 2021 T-ORT model from 15 Hz OBN TLFWI. The 6-azimuth Kirchhoff gathers (d)-(f) from the OBN data (max offset 8 km) using the models in (a)-(c), respectively. White vertical lines on the tops of the model displays indicate gather locations.

10.1190/image2022-3751236.1

After updating the azimuthal anisotropy, 15 Hz T-ORT TLFWI was carried out to further improve the velocity model with better constraints from the full-azimuth OBN data and more accurate orthorhombic wave propagation. The 15 Hz TLFWI model has better resolution of the shallow anomalies (Figure 4). The 6-azimuth OBN Kirchhoff gathers migrated with the 2019 T-ORT model addressed major orthorhombic effects at top reservoir level when compared to the TTI models. However, some fine details were still missing to fully flatten the gathers, which was resolved by the 2021 OBN T-ORT TLFWI model.

In addition to the velocity update, a Q model that represents the anelastic attenuation effects was also estimated by QFWI (Wang et al., 2018) using the OBN data. Subsequent imaging algorithms can use the Q model to compensate for the severe attenuation introduced by the shallow absorption bodies.

FWI Imaging

A two-iteration LS-Kirchhoff (Zhu et al., 2018) with OBN downgoing, OBN upgoing, and NAZ data was performed to obtain a combined high-resolution image. A single-iteration LSRTM (Wang et al., 2016) with OBN downgoing data was also performed to obtain a structural image. Both migrations were Q-compensated with the Q model estimated by QFWI. Although better illumination was observed in both LS migrations compared to conventional migrations, some key areas still lacked the details for reservoir development. In complex geological settings such as Trion, the Kirchhoff algorithm usually falls short due to raytracing difficulties and is hindered by the essential drawback of single-arrival imaging. RTM performs better than Kirchhoff with complex velocity, but illumination is still poor. One or two iterations of least-squares migration cannot fully compensate for the illumination issues at the Trion reservoir.

FWI Imaging (Zhang et al., 2020) is an emerging imaging algorithm for structural interpretation with several successful applications (Liu et al., 2021; Wray et al., 2021). FWI Imaging applies iterative least-squares fitting to the full-wavefield data, including transmission waves, primary reflections, and their multiples, which leads to images with additional structural information, more balanced illumination, and higher S/N ratio (Huang et al., 2021).

In this study, the maximum frequency of the TLFWI was pushed to 25 Hz to generate an FWI Image with comparable frequency to the LSRTM. The same Q model used for LS-Kirchhoff and LSRTM was employed in TLFWI for FWI Imaging. Figure 5 compares LS-Kirchhoff, LSRTM, and FWI Imaging results in the north and west areas of the Trion field. FWI Imaging shows better illumination and higher S/N at the shallow folding structure and down to the Mesozoic level compared to the images from LS-Kirchhoff and LSRTM. The single-arrival Kirchhoff migration suffers from ray-tracing drawbacks under complex velocity provided worst structure image (Figure 5a, 5d). In Figure 6, a fence line is displayed comparing the FWI Image to LS-Kirchhoff and LSRTM images. In this example, we applied a 25 Hz low-pass filter to the LS-Kirchhoff and LSRTM results so that similar frequencies are compared. The trough amplitude at the top of the reservoir was extracted for comparison (Figures 6d-f). The FWI Image shows more coherent events than the LS-Kirchhoff and LSRTM across the whole section, especially around the center left part, which is close to the shallow absorption body where the images from LS-Kirchhoff and LSRTM are weak. The top reservoir amplitude extraction from the FWI Image exhibits better coherence and S/N than those from LS-Kirchhoff and LSRTM. The structural and amplitude information from the FWI Image filled the gaps left by LS-Kirchhoff and LSRTM.

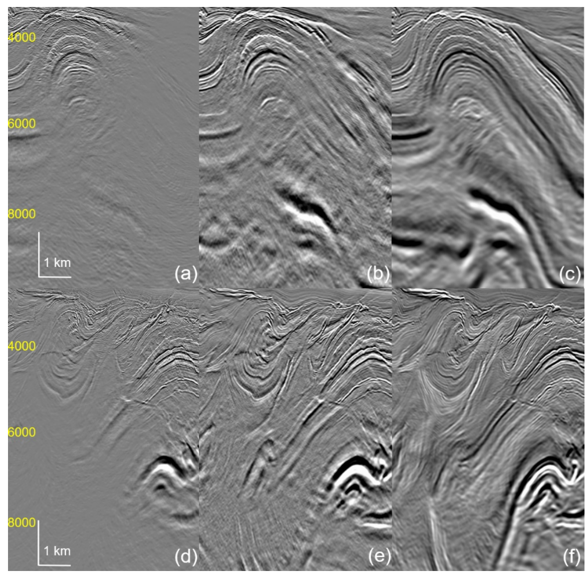

Figure 5: (a) LS-Kirchhoff, (b) LSRTM, and (c) FWI Image north of the Trion field; (d) LS-Kirchhoff, (e) LSRTM, and (f) FWI Image west of the Trion field. The FWI Image has better illumination for steep events and higher S/N in the deep section benifiting from iterative LS data fitting and additional illuminations from diving waves and multiples.

Discussion and conclusions

The OBN data and TLFWI were the two major contributing factors for a successful velocity update at Trion. The OBN data provided long-offset and low-frequency information, which are essential for FWI. The TLFWI-updated T-ORT models resolved the azimuthal anisotropy better than earlier approaches using streamer data. The OBN TLFWI provided a high-resolution velocity field, which helped to generate an improved image over LS-Kirchhoff and LSRTM. However, even with improved T-ORT models, the LS migrations are still not able to fully image all the structures at Trion and weak amplitude zones remain in poorly illuminated areas. FWI Imaging, which leverages an iterative data fitting process of the full wavefield, provided better illumination compensation and more balanced amplitudes, resulting in a more accurate reservoir image.

Despite the improvements in image quality, a few challenges remain. To obtain an FWI Image with comparable frequency to Kirchhoff is cost prohibitive. Moreover, insufficient (acoustic modeling engine instead of elastic) and inaccurate physics (uncertainties in density, absorption, and anisotropy) could contaminate the inverted velocity model, especially towards high frequencies.

This study demonstrated that there are a lot of useful information that can be extracted from OBN data with the proper technology. With a TLFWI velocity and FWI Image, the current OBN product provided better structural and amplitude information than what could be obtained from streamer processing. As technology evolves to a more advanced stage, the uncertainty at the Trion reservoir can be further reduced.

Acknowledgments

We thank BHP, Pemex, and CGG for permission to publish this work.

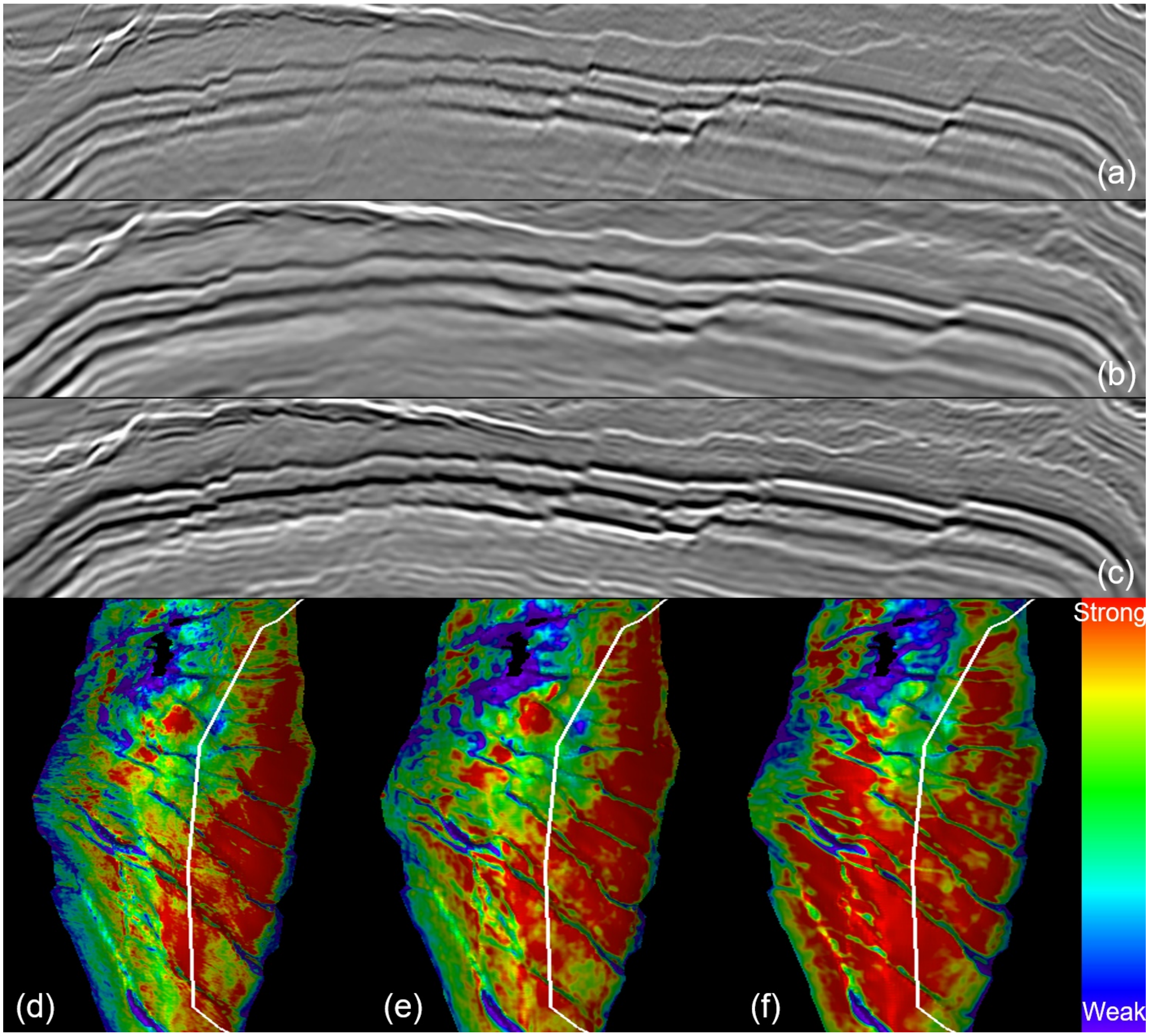

Figure 6: Fence line view for (a) LS-Kirchhoff, (b) LSRTM, and (c) FWI Image. A 25 Hz low-pass filter was applied to (a) and (b). (d)-(f) are the trough amplitude extractions at the reservoir top for LS-Kirchhoff, LSRTM, and FWI Image, respectively, with the fence line location indicated by the white lines overlaid.

10.1190/image2022-3751236.1

REFERENCES

Ahmed, I., 2018, Diving wave illumination using RTM to analyze acquisition geometries for FWI: 88th Annual International Meeting, SEG, Expanded Abstracts, 1299–1303, doi: https://doi.org/10.1190/segam2018-2997116.1.

Huang, R., Z. Zhang, Z. Wu, Z. Wei, J. Mei, and P. Wang, 2021, Full-waveform inversion for full-wavefield imaging: Decades in the making: The Leading Edge, **40**, no. 5, 324–334, doi: https://doi.org/10.1190/tle40050324.1

Liu, J., M. Yang, J. Deeds, J. Luckow, T. Cheriyan, P. Ariston, Z. Yang, M. Mei, and Z. Zhang, 2021, Solving subsalt imaging challenges in Green Canyon using OBN and FWI Imaging: First International Meeting for Applied Geoscience & Energy, SEG/AAPG, Expanded Abstracts, 727–731, doi: https://doi.org/10.1190/segam2021-3583443.1

Nolte, B., F. Rollins, Q. Li, S. Dadi, S. Yang, J. Mei, and R. Huang, 2019, Salt velocity model building with FWI on OBN data: Example from Mad Dog, Gulf of Mexico: 89th Annual International Meeting, SEG, Expanded Abstracts, 1275–1279, doi: https://doi.org/10.1190/segam2019-3216777.1.

Schuster, G. T., 1993, Least-squares cross-well migration: 63rd Annual International Meeting, SEG, Expanded Abstracts, 110–113, doi: https://doi.org/10.1190/1.1822308.

Shao, G., X. Zhao, Q. Tong, R. Huang, D. Baptiste, L. Jiang, and B. Nolte, 2020, FWI-driven orthorhombic modeling with OBS data for reservoir imaging offshore Trinidad: 90th Annual International Meeting, SEG, Expanded Abstracts, 745–749, doi: https://doi.org/10.1190/segam2020-3427205.1.

Tsvankin, I., 1997, Anisotropic parameters and P-wave velocity for orthorhombic media: Geophysics, **62**, 1292–1309, doi: https://doi.org/10.1190/1.1444231.

Wang, M., Y. Xie, B. Xiao, A. Ratcliffe, and T. Latter, 2018, Visco-acoustic full-waveform inversion in the presence of complex gas clouds: 88th Annual International Meeting, SEG, Expanded Abstracts, 5516–5520, doi: https://doi.org/10.1190/segam2018-w23-01.1.

Wang, P., A. Gomes, Z. Zhang, and M. Wang, 2016, Least-squares RTM: Reality and possibilities for subsalt imaging: 86th Annual International Meeting, SEG, Expanded Abstracts, 4204–4209, doi: https://doi.org/10.1190/segam2016-13867926.1.

Wang, P., Z. Zhang, J. Mei, F. Lin, and R. Huang, 2019, Full-waveform inversion for salt: A coming of age: The Leading Edge, **38**, 304–213, doi: https://doi.org/10.1190/tle38030204.1.

Wray, B., L. Zheng, F. Rozario, X. Zhang, N. Chazalnoel, and C. Mifflin, 2021, Paradigm shift: Recent advances in model building and imaging at Shenzi: First International Meeting for Applied Geoscience & Energy, SEG/AAPG, Expanded Abstracts, 572–576, doi: https://doi.org/10.1190/segam2021-3580654.1.

Yao, Y., H. Zhang, L. Hu, and C. Peng, 2020, Improving Mississippi Canyon images with ocean bottom node data: Challenges and surprises: 90th Annual International Meeting, SEG, Expanded Abstracts, 661–665, doi: https://doi.org/10.1190/segam2020-3423896.1.

Zhang, Z., J. Mei, F. Lin, R. Huang, and P. Wang, 2018, Correcting for salt misinterpretation with full-waveform inversion: 88th Annual International Meeting, SEG, Expanded Abstracts, 1143–1147, doi: https://doi.org/10.1190/segam2018-2997711.1.

Zhang, Z., Z. Wu, Z. Wei, J. Mei, R. Huang, and P. Wang, 2020, FWI Imaging: Full-wavefield imaging through full- waveform inversion: 90th Annual International Meeting, SEG, Expanded Abstracts, 656–660, doi: https://doi.org/10.1190/segam2020-3427858.1.

Zhu, H., M. Al-Waily, Z. Chang, and Z. Yang, 2018, Using least-squares Kirchhoff migration for better shallow imaging of spatially sparse dual-WAZ data: 88th Annual International Meeting, SEG, Expanded Abstracts, 4321–4325, doi: https://doi.org/10.1190/segam2018-2995491.1.